

What does the CMS measurement of W-polarization tell us about the underlying theory of the coupling of W-bosons to matter?

Alexander Belyaev^{a,b} and Douglas Ross^a

^a*School of Physics & Astronomy, University of Southampton, Highfield, Southampton SO17 1BJ, U.K.*

^b*Particle Physics Department, Rutherford Appleton Laboratory, Chilton, Didcot, Oxon OX11 0QX, U.K.*

E-mail: a.belyaev@soton.ac.uk, d.a.ross@soton.ac.uk

ABSTRACT: We discuss results of the CMS collaboration on the sensitivity of the LHC to W boson polarisation in the process $pp \rightarrow W^\pm + \text{jet} \rightarrow e^\pm \text{jet} + \cancel{P}_T$ using the L_P variable directly connected to θ^* angle of the outgoing lepton in the rest frame of the decaying W . We have shown that for a given L_P , interference between different polarizations of the W -boson is not negligible, and needs to be taken into account when considering the differential cross-section with respect to L_P . The L_P variable suggested by CMS collaboration is highly suitable variable to study LHC sensitivity to g_V, g_A couplings of W -boson to fermions. We note that the experimental sensitivity to W -boson polarization which is much higher than that to (g_V, g_A) parameter space can be turned around and used to identify deviations from the Standard Model as a signal for new physics at the LHC.

KEYWORDS: Standard Model, Beyond Standard Model

Contents

1	Introduction	1
2	LHC sensitivity to the process $pp \rightarrow W^\pm + \text{jet} \rightarrow e^\pm + \text{jet} + \cancel{P}_T$	3
2.1	Setup for our analysis	3
2.2	L_P variable	4
2.3	The value of the W -boson interference for L_P variable	5
2.4	LHC sensitivity to $g_A - g_V$ parameter space	9
3	Conclusions	12

1 Introduction

The CMS collaboration [1] has performed a measurement of the distribution of positive, (f_+), negative, (f_-), and longitudinal, (f_0), polarisations of the W -boson in the process

$$pp \rightarrow \text{jet} + W^\pm \rightarrow \text{jet} \ell^\pm \nu \tag{1.1}$$

for $\ell^\pm = e^\pm$ and μ^\pm . Such an analysis is possible if one can measure the polar, θ^* and azimuthal, ϕ^* angles of the outgoing lepton in the rest frame of the decaying W (relative to an axis defined by the direction of the W in the incoming CM frame).

Since the experiment only observes the decay products of the W in the laboratory frame (as opposed to the rest-frame of the W), one cannot, in general, neglect the effect of interference between the production/decay amplitudes for a W of different polarization. In other words, the polarization of the W -boson is *not* an observable. Nevertheless, in terms of the angles θ^*, ϕ^* defined above the differential cross section (in the case of W^-) may be written as

$$\begin{aligned} \sigma \frac{d^2\sigma}{d\cos\theta^* d\phi^*} = \frac{1}{4\pi} \left\{ f_+ \frac{(1 - \cos\theta^*)^2}{2} + f_- \frac{(1 + \cos\theta^*)^2}{2} + f_0 (1 - \cos\theta^*)^2 \right. \\ \left. + \sqrt{2}g_{+0} \sin\theta^* (1 - \cos\theta^*) \cos\phi^* - \sqrt{2}g_{-0} \sin\theta^* (1 + \cos\theta^*) \cos\phi^* \right. \\ \left. - g_{+-} \sin^2\theta^* \cos(2\phi^*) \right\} \tag{1.2} \end{aligned}$$

where f_i are the probabilities for the production and decay of a W^- with polarization i whereas g_{ij} are the interferences of the amplitudes for production and decay between W^- with polarizations i and j . We see from eq. (1.2) that after integration over the azimuthal angle, the interference terms vanish and one can indeed extract the probabilities for the production of the three possible polarizations from the differential cross-section

w.r.t. $\cos\theta^*$. Here we neglect “T-odd” contributions at higher order QCD (see e.g. [2, 3] and references therein).

Unfortunately $\cos\theta^*$ distribution cannot be measured directly. One needs to find the longitudinal component of the neutrino from W -boson decay first which is not measured but can be deduced from missing transverse momentum, \cancel{P}_T , the electron momentum, p_e , together with the assumption that the process goes through the production of an on-shell W -boson. However, this deduction leads to a quadratic equation with two solutions for the longitudinal neutrino momentum, p_Z^ν . Therefore $\cos\theta^*$ cannot in general be measured unambiguously. However, the variable L_p (discussed below), proposed in [1] which closely matches $\cos\theta^*$ for W -bosons with the large transverse momentum.¹

Using this variable the analysis of W -polarizations has been performed and the sensitivity of the LHC to W -polarization was derived.

We make the point here that since the variable, L_p does not exactly match $\cos\theta^*$, even at very high $p_T(W)$, one should describe the differential cross-section $d\sigma/dL_P$ in terms of the sum of contributions from the production of W -bosons with given helicity taking into account corrections arising from the interference between intermediate W -bosons of different helicity.

In ref. [1], templates were constructed from re-weightings necessary to produce dependencies on $\cos\theta^*$ from purely left-, right-, or longitudinally polarized W -bosons, and translating this into differential cross-sections in terms of the variable, L_P . The interference coefficients, g_{ij} were taken to be those for the SM and the effect of varying the magnitude of these by $\pm 10\%$ was investigated and included in the systematic error quoted on the measured values of f_i [5].

In this paper, we take an orthogonal, but complementary approach - namely we recalculate the differential cross-section with respect to L_P and examine quantitatively the contribution from the interference terms. We then look at the effect of altering the vector, g_V , and axial-vector, g_A , couplings of the W -bosons to quarks, in order to investigate the extent to which the results quoted in ref. [1] can be used to identify deviations from the Standard Model as a signal for new physics in the structure of weak interactions. In our analysis, we do not extract values for the f_i as we cannot disentangle the interference contributions. We find that for any of the partonic sub-processes contributing to the process (1.1), there is indeed a sizeable interference effect, but for reasons that must be coincidental (the three partonic sub-processes are folded with independent parton-distribution functions), the overall effect is suppressed owing to the fact that the dominant partonic sub-process is the one for which the interference is smallest. Nevertheless, the remnant interference effect is of the order of the statistical experimental errors quoted in ref. [1] and presumably significantly larger than the current error bars that would be extracted from an analysis over the current (and future) entire integrated luminosity. For future analysis of W -boson helicity distributions, with improved statistics, it would be advisable to account directly

¹The ATLAS collaboration [4] has performed a similar analysis using a different directly measurable variable, θ_{2D} , which matches θ^* when the transverse momentum of the W -boson dominates its longitudinal momentum.

for interference, or alternatively to use templates in which the interference coefficients, g_{ij} , are also parameters to be fitted.

Since interference cannot be neglected, rather than extracting the probabilities, f_i , one should simply parameterize the weak interactions in terms of the couplings, g_V and g_A . We show that the differential cross section $d\sigma/dL_P$ is not very sensitive to changes in g_V and/or g_A , but rather the 68% and 95% CL contours engulf a rather large region in the $g_V - g_A$ plane. Thus, although the results reported in [1] lead to a measurement of the probabilities f_i to a high degree of accuracy, we find that the accuracy to which the vector and axial vector couplings are measured is considerably poorer. We emphasize that it is the accuracy to which the LHC can determine these couplings, rather than the distribution of polarizations of the W -boson, that provides direct sensitivity to the underlying theory (i.e. sensitivity to deviations from the Standard Model).

The values of g_V and g_A have previously been extracted from weak decays at low energies and shown to be consistent with the Standard Model (SM). If there is new physics beyond the standard model, then the effect of such new physics on the effective values of these couplings is likely to be energy dependent, so that it is informative to compare the values extracted at low-energy weak interactions with those measured for on-shell W -bosons.

In this paper we plot the domain of g_V and g_A couplings extracted from the angular distributions in W -boson production and decay at the LHC and show that whereas it is compatible with the SM result, there remains a considerable range for the ratio g_A/g_V which is still compatible with data.

This paper is organised as follows. In section 2 we provide details on the W -boson interference contributing to $d\sigma/dL_P$ and estimate LHC accuracy to measure the vector and axial vector couplings. In section 3 we draw our conclusions.

2 LHC sensitivity to the process $pp \rightarrow W^\pm + \text{jet} \rightarrow e^\pm + \text{jet} + \cancel{P}_T$

2.1 Setup for our analysis

To explore the LHC sensitivity for the process $pp \rightarrow W^\pm + \text{jet} \rightarrow e^\pm + \text{jet} + \cancel{P}_T$, we have evaluated the helicity amplitudes for this process and have created the respective Monte-Carlo parton-level generator linked to PYTHIA [6, 7] to simulate effects beyond the parton-level including as well as effects related to detector-energy resolution. This generator is also able to produce events in the Les Houches Accord format [8] (LHE) which we have used to link to the PGS [9] fast detector simulation package.

Our study was done at the leading order and was concentrated on effects related to W -boson polarisation and LHC sensitivity to W -boson couplings to matter.

In our calculation we have used:

1. CTEQ6L PDF evaluated at the scale $Q^2 = E_T^2(W) \equiv M_W^2 + (p_T(W))^2$, choosing the renormalisation and factorisation scale equal to each other;
2. $\alpha_s(M_Z) = 0.1184$, $\alpha_{em}(M_Z) = 0.007818$. To be specific, in our analysis we have concentrated on the e^- channel and have used kinematic cuts specific for the electron

Cut #	Cut value
<i>Cut 1</i>	$p_T(W) > 50 \text{ GeV}$
<i>Cut 2</i>	$p_T(e) > 25 \text{ GeV}, \eta(e) < 2.4$
<i>Cut 3</i>	Electron isolation within the cone $\Delta R = 0.3$
<i>Cut 4</i>	Transverse mass of W , $M_{W}^T, > 50 \text{ GeV}$

Table 1. The set of kinematic cuts applied for the process $pp \rightarrow W^\pm + \text{jet} \rightarrow e^\pm + \text{jet} + \cancel{P}_T$.

signature. One should note that an analysis for e^+ channel as well as for the muon channel are qualitatively similar and lead to the same qualitative conclusions.

We have taken into account contribution from $q = u, d, s, c$ flavours into the process $pp \rightarrow W^\pm + \text{jet} \rightarrow e^\pm + \text{jet} + \cancel{P}_T$ which consists of the following 3 (partonic) subprocesses for $W^- + \text{jet}$ production:

- a) $q_d \bar{q}_u \rightarrow g e^- \bar{\nu}_e$
- b) $\bar{q}_u g \rightarrow \bar{q}_d e^- \bar{\nu}_e$
- c) $q_d g \rightarrow q_u e^- \bar{\nu}_e$

and 3 analogous subprocesses for $W^+ + \text{jet}$ production.

For the analysis we have used the same set of kinematic cuts which has been used by CMS collaboration in [1] and which we have summarised in table 1.

After the *Cut 1* the LO cross section for the process $pp \rightarrow W^- + \text{jet} \rightarrow e^- \text{jet} + \cancel{P}_T$ ($pp \rightarrow W^+ + \text{jet} \rightarrow e^+ \text{jet} + \cancel{P}_T$) is equal to 127.3 (202.7) pb which has provided about 4.6×10^3 (7.3×10^3) events for 36 pb^{-1} integrated luminosity analysed by CMS in [1] @ 7 TeV LHC. For the total integrated luminosity about 20 fb^{-1} at the latest LHC run @ 8 TeV, the number of expected events is almost 2 orders of magnitude larger providing an excellent framework for improvement of the LHC sensitivity to W -boson polarization and couplings to matter.

2.2 L_P variable

To be able to measure polarisation of W -boson and its couplings to matter one should be able to access $\cos \theta^*$ value, which, as we have mentioned above cannot be extracted unambiguously. Instead, ref. [1] have proposed the variable L_P defined by

$$L_P = \frac{\mathbf{p}_T(e) \cdot \mathbf{p}_T(W)}{|\mathbf{p}_T(W)|^2}, \tag{2.1}$$

where $\mathbf{p}_T(e)$, $\mathbf{p}_T(W)$ are the transverse momenta of the outgoing charged lepton and the W respectively. In terms of the polar and azimuthal angles θ^* , ϕ^* the variable L_P is given by²

$$L_P = \frac{1}{2} + \frac{1}{2} \frac{(\hat{s} + M_W^2)}{(\hat{s} - M_W^2)} \cos \theta^* \pm \frac{M_W \sqrt{\hat{s}}}{(\hat{s} - M_W^2)} \frac{|\mathbf{p}_{||}(W)|}{|\mathbf{p}_T(W)|} \sin \theta^* \cos \phi^* \tag{2.2}$$

²In this paper we restrict our analysis to the case of a single (narrow) jet accompanying the W -boson,

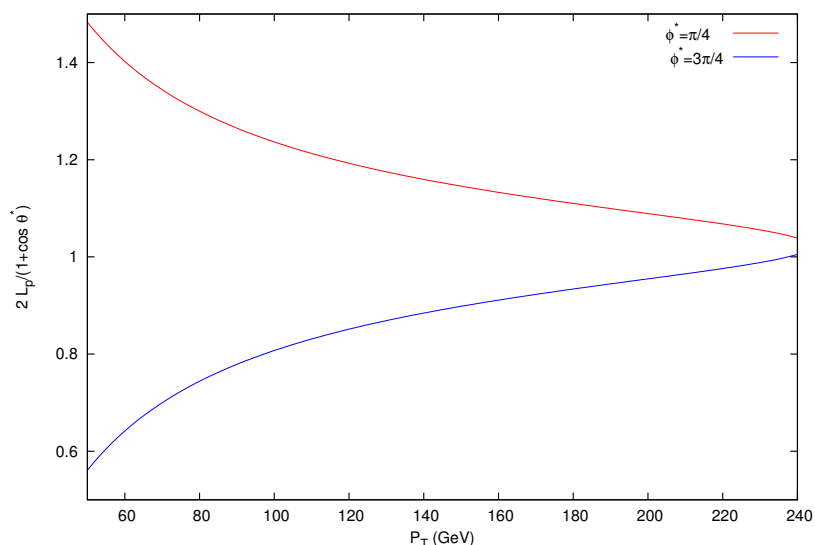


Figure 1. The ratio of L_P to $\frac{1}{2}(1 + \cos \theta^*)$ against the transverse momentum of the W for azimuthal angles $\phi^* = \pi/4$ and $\phi^* = 3\pi/4$. We have taken $\theta^* = \pi/4$ and $\sqrt{\hat{s}} = 0.5$ TeV.

where \hat{s} is the invariant square-mass of the W +jet and the related quantity $|\mathbf{p}_{||}(W)|$ is the longitudinal component of the momentum of the W . For sufficiently large $|\mathbf{p}_{\mathbf{T}}(W)|$ eq. (2.2) may be approximated by

$$L_P \approx \frac{1}{2}(1 + \cos \theta^*), \tag{2.3}$$

so that if a sufficiently large minimum cut is imposed on $|\mathbf{p}_{\mathbf{T}}(W)|$, the (ambiguous) dependence of L_P on the azimuthal angle ϕ^* decouples so that the differential cross-section w.r.t. L_P can be used to extract the probabilities for the different W polarisations.

However, it can be seen from figure 1 that this approximation is only valid at very high values of $|\mathbf{p}_{\mathbf{T}}(W)|$ and that even for $|\mathbf{p}_{\mathbf{T}}(W)| = 240$ GeV (close to the kinematic limit for $\sqrt{s} = 500$ GeV) there is a 5% difference. In ref. [1], the cut imposed on $|\mathbf{p}_{\mathbf{T}}(W)|$ was 50 GeV, where we can see that there are very large corrections to the approximation (2.3). For this figure we have chosen 500 GeV as the partonic subenergy, $\sqrt{\hat{s}}$ since for higher $\sqrt{\hat{s}}$ the contribution to the total cross section is below 1% at 7 TeV LHC.

Consequently, we expect a significant contribution to the cross-section $d\sigma/dL_P$ from interference terms - i.e. it is *not* a good approximation to assume that the dependence on ϕ^* factorises in such a way that the effect of interference on this differential cross-section is small.

2.3 The value of the W -boson interference for L_P variable

In figure 2 we present $d\sigma/dL_P$ distributions for an individual subprocesses contributing to the process $pp \rightarrow W^- + \text{jet} \rightarrow e^- \text{jet} + \cancel{p}_T$ after *Cut 1* (see table 1) at 7 TeV LHC, 36 pb⁻¹ (left column) and 14 TeV LHC, 100 fb⁻¹ (right column). One can see that the relative interference effect can be above 10% in the case of the process $q_d \bar{q}_u \rightarrow g e^- \bar{\nu}_e$ and clearly cannot be neglected.

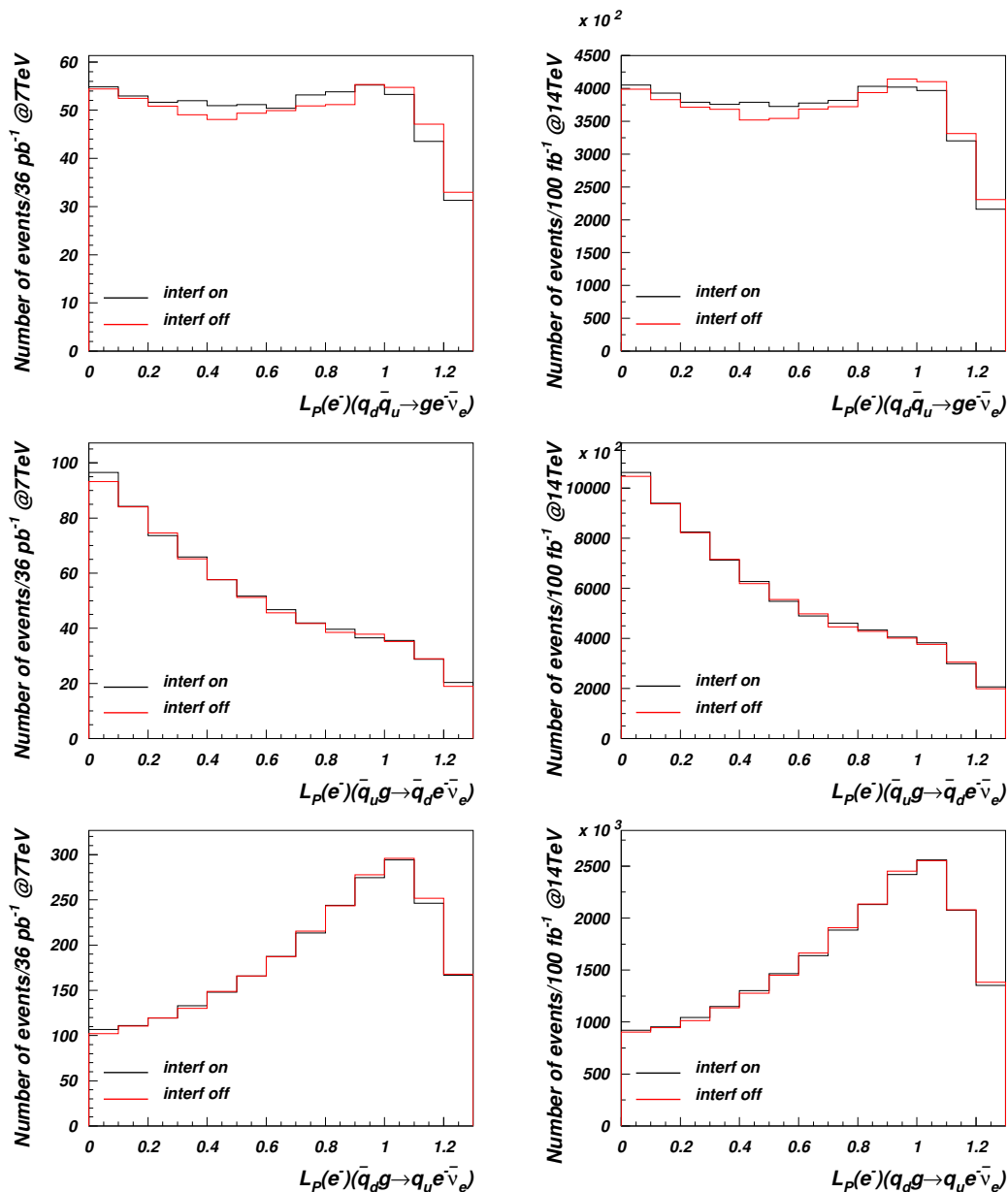


Figure 2. The effect of the interference of the W – boson polarisations for L_P variable for individual subprocesses at 7 TeV LHC, 36 pb^{-1} (left column) and 14 TeV LHC, 100 fb^{-1} (right column). Black line — interference is taken into account, red line — interference is neglected.

This is the case for both 7 TeV and 14 TeV LHC energies. At the same time one can see that the process $q_d \bar{q}_u \rightarrow g e^- \bar{\nu}_e$ is not the dominant one; the main contribution to the process $pp \rightarrow W^\pm + \text{jet} \rightarrow e^- \text{jet} + \cancel{P}_T$ actually comes from the subprocess $q_d g \rightarrow q_u e^- \bar{\nu}_e$. Therefore, the overall effect of interference in $d\sigma/dL_P$ distribution is only at a few percent level as we present in detail below. So accidentally, the overall interference effect turns out to be quite small, for most of the L_P bins, but nevertheless not negligible. The situation is qualitatively the same for the process $pp \rightarrow W^+ + \text{jet} \rightarrow e^+ \text{jet} + \cancel{P}_T$.

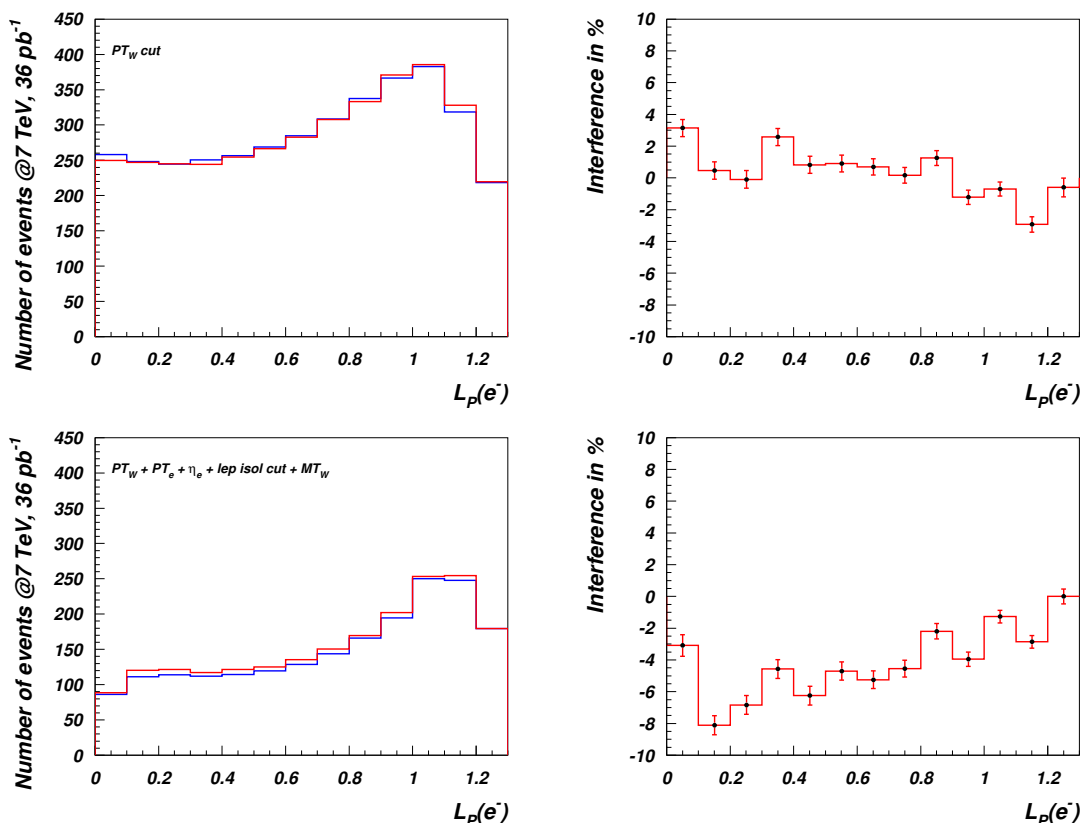


Figure 3. Overall interference effect of W -boson polarisations in $d\sigma/dL_P$ 7 TeV LHC with 36 pb^{-1} after the consequent application of the kinematic cuts from table 1 for the process $pp \rightarrow W^- + \text{jet} \rightarrow e^- \text{jet} + \cancel{P}_T$. Left: distribution with (blue) and without (red) interference. Right: the relative value of the interference versus dL_P including Monte-Carlo statistical error. Upper: distributions after Cut 1, Lower: distributions after Cuts 1-4.

Let us take a look at the overall interference effect after the consequent application of the kinematic cuts from table 1 presented in figure 3-3. In these figures we present total $d\sigma/dL_P$ distributions at 7 TeV LHC with 36 pb^{-1} for the processes $pp \rightarrow W^- + \text{jet} \rightarrow e^- \text{jet} + \cancel{P}_T$ (figure 3) and $pp \rightarrow W^+ + \text{jet} \rightarrow e^+ \text{jet} + \cancel{P}_T$ (figure 4), but ignoring effects of calorimeter energy smearing, trigger efficiency as well as effects of jet fragmentation.

One can see here that the total interference can be as large as about 10% in certain bins of $d\sigma/dL_P$ distribution which one can observe from the right and middle parts of figure 3 and figure 4 respectively. Another observation is that while kinematic cuts suppress overall event rate, they do not visibly affect the magnitude of the interference, so that the relative importance of such interference increases as more and more cuts are applied. For low L_P values it reaches -8% in certain bins for 7 TeV collision. One should also mention that for the process $pp \rightarrow W^+ + \text{jet} \rightarrow e^+ \text{jet} + \cancel{P}_T$ the interference is smaller than for $pp \rightarrow W^- + \text{jet} \rightarrow e^- \text{jet} + \cancel{P}_T$ production. From this point we will be presenting results only for the process $pp \rightarrow W^- + \text{jet} \rightarrow e^- \text{jet} + \cancel{P}_T$ recalling that the results for $pp \rightarrow W^+ + \text{jet} \rightarrow e^+ \text{jet} + \cancel{P}_T$ one are qualitatively the same.

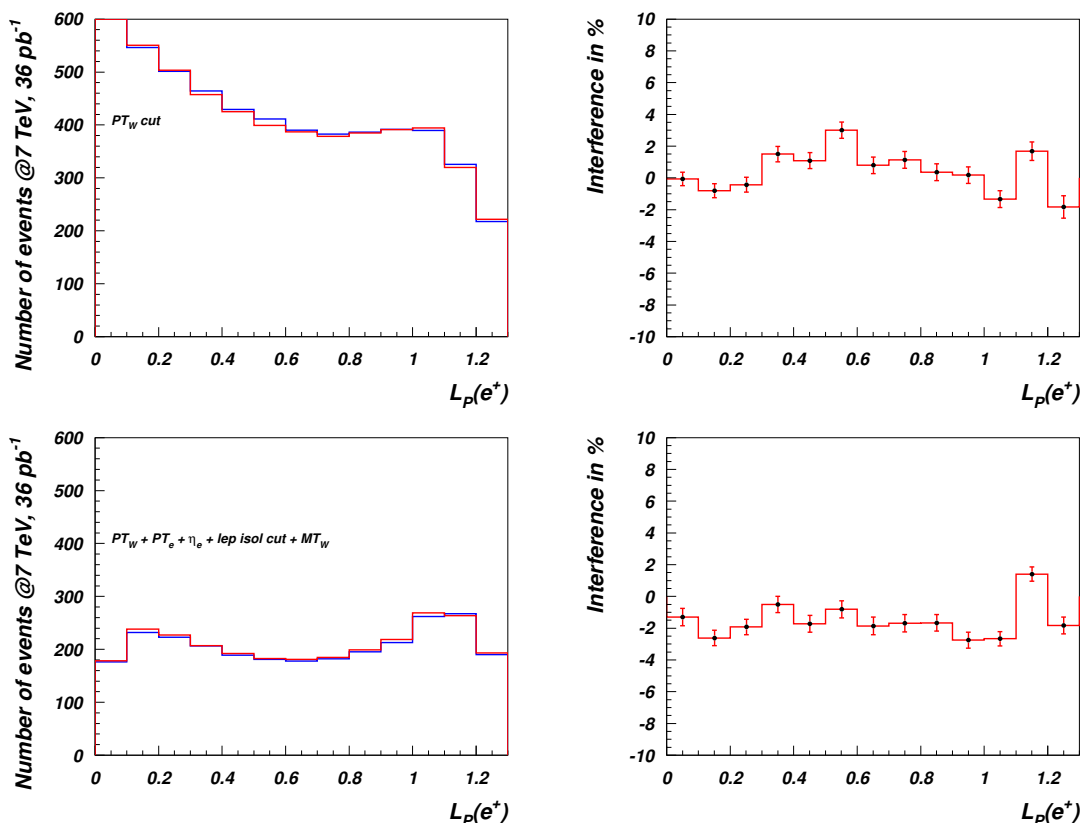


Figure 4. Overall interference effect of W -boson polarisations in $d\sigma/dL_P$ 7 TeV LHC with 36 pb^{-1} after the consequent application of the kinematic cuts from table 1 for the process $pp \rightarrow W^+ + \text{jet} \rightarrow e^+ + \text{jets} + \cancel{P}_T$. Left: distribution with (blue) and without (red) interference. Right: the relative value of the interference versus dL_P including Monte-Carlo statistical error. Upper: distributions after *Cut 1*, Lower: distributions after *Cuts 1-4*.

We have examined the sensitivity of the predicted differential cross-sections to different CTEQ PDF sets. The total cross-section differs by around 5% between different sets, but the shape of the distribution in L_P is fairly insensitive, i.e. if we renormalize so that the total cross-sections agree, the difference between the differential cross-sections in any L_P bin is less than 2% and therefore significantly lower than the effect of interference for most of the range of L_P for the case of W^- production. In this paper we used the CTEQ6L set as this was the set used in ref. [1].

In figure 5 we present analogous results for 14 TeV LHC with 100 fb^{-1} for the process $pp \rightarrow W^- + \text{jet} \rightarrow e^- \text{jet} + \cancel{P}_T$. One can see that the shape of the interference for the L_P distribution does not change, however its relative size decreases down to about 6% for low L_P bin. This is expected since at higher energies the $P_T(W)$ distribution is shifted to the higher end, which makes the approximation (2.3) more accurate - recalling that the interference effects cancel completely in the limit where eq. (2.3) becomes exact.

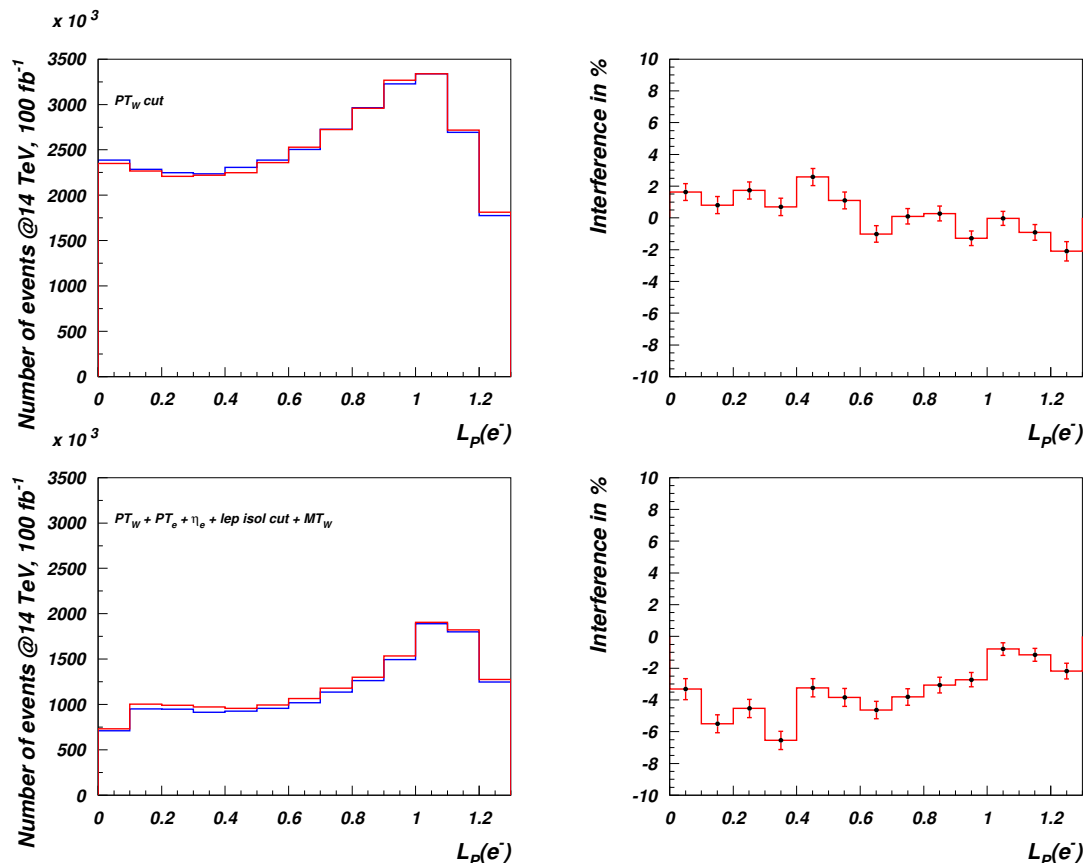


Figure 5. Overall interference effect of W -boson polarisations in $d\sigma/dL_P$ 14 TeV LHC with 100 pb^{-1} after the consequent application of the kinematic cuts from table 1. Left: distribution with (blue) and without (red) interference. Right: the relative value of the interference versus L_P including Monte-Carlo statistical error. Upper: distributions after *Cut 1*, Lower: distributions after *Cuts 1-4*.

2.4 LHC sensitivity to $g_A - g_V$ parameter space

The CMS collaboration has studied sensitivity of the LHC to measure the W -boson polarisation ([1]), however this sensitivity does not provide a clear information about underlying theory. On the other hand, the fit of L_P distribution as we show below could provide the measurement of axial and vector couplings of W -boson to fermions making therefore a connection to the underlying Lagrangian.

In this subsection we study the LHC sensitivity g_A, g_V couplings of W -boson. In figure 6(left) we present $L_P(e^-)$ distributions for $g_A = g_V = 1$ (SM) case (red line) as well as for $g_A = 0, g_V = \sqrt{2}$ case represented by the blue line. These distributions ignore the effects of calorimeter energy smearing, trigger efficiency as well as effects of jet fragmentation but do include the application of Cuts 1-4. Using these distributions we made an attempt to fit experimental data (including experimental errors) from [1] with g_A, g_V . First of all, one can see that at such level of simulation our $L_P(e^-)$ prediction describes data quite well — it is only above data by about 10%, which is also indicated in the best values of g_V and g_A : $g_A^* = g_V^* = 0.86 \pm 0.5$. Also in the right panel of figure 6 we present 67% and

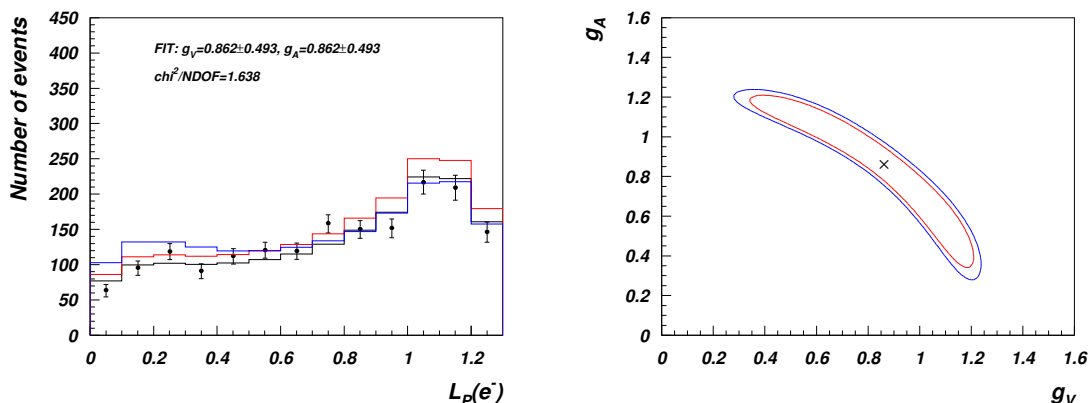


Figure 6. Left: Data (black dots) fit (solid black) with L_P distributions (red is for $g_A = g_V = 1$, blue is for $g_A = 0, g_V = \sqrt{2}$). Right: 67% (red) and 95% (blue) confidence level contours for the respective fit. Effects of calorimeter energy smearing, trigger efficiency as well as effects are ignored.

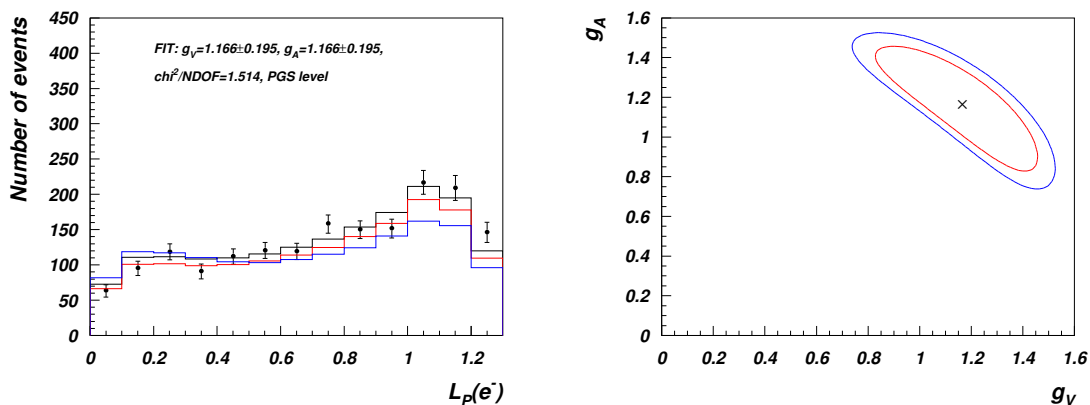


Figure 7. Left: Data (black dots) fit (solid black) with PGS (fast detector level simulation) L_P distributions (red is for $g_A = g_V = 1$, blue is for $g_A = 0, g_V = \sqrt{2}$). Right: 67% (red) and 95% (blue) confidence level contours for the respective fit.

95% confidence level contours for this fit. One can see that the sensitivity to the values of g_A, g_V is quite low. One should note, that the contour plot in figure 6(right) reflects a clear correlation between g_A and g_V parameters while the error of the fit is reflected in the respective maximal variation of either parameter g_A or g_V at the 67% confidence level.

In the next stage we have performed fast detector simulation using the PGS package [9]. At this level we have taken into account effects of calorimeter energy smearing, trigger efficiency as well as effects of jet fragmentation.

In figure 7(left) we present $L_P(e^-)$ distributions for $g_A = g_V = 1(SM)$ case (red line) as well as for $g_A = 0, g_V = \sqrt{2}$ case (represented by the blue line) analogous to the previous figure but after the use of the PGS package.

One can see that PGS slightly affect the shape of the L_P distribution: the distribution for $L_P \geq 1$ is somewhat more suppressed than the region of lower L_P . Noting that this region is dominated by low $p_T(W)$ and respectively low p_T of its decay products and

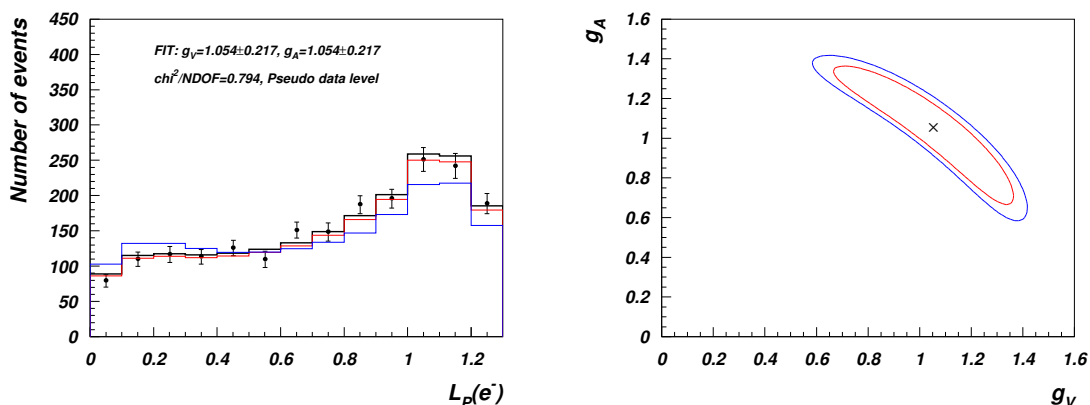


Figure 8. Left: “Pseudo data” (randomised $g_A = g_V = 1$ distribution — black dots) fit with “parton level” L_P distributions (red is for $g_A = g_V = 1$, blue is for $g_A = 0, g_V = \sqrt{2}$). Right: 67% (red) and 95% (blue) confidence level contours for the respective fit.

associated jets, this indicates that under more realistic conditions the low p_T events have slightly lower detector efficiency.³

One can see that now, the $g_A = g_V = 1$ case provides even better quantitative description of data, which is indicated in the fitted values of $g_A^* = g_V^* = 1.17 \pm 0.20$ as well as slightly better value of χ^2 . The respective sensitivity in $g_A - g_V$ plane is indicated in figure 7(right).

The full detector simulation would provide the ultimate level of data description, therefore, assuming this, we have randomised results for our L_P distribution around their mean values according to the Gaussian distribution using available experimental errors. Using this “pseudo data” level of analysis we have estimated the LHC sensitivity to g_V, g_A parameters presented in figure 8 in analogy to the previous ones. One can see that in comparison with the approaches above, we have achieved slightly better χ^2 fit and the the sensitivity to g_V, g_A parameters ($g_A^* = g_V^* = 1.02 \pm 0.16$).

For all three methods of analysis above which are in a good agreement between each other, one can see the LHC sensitivity to g_V, g_A parameters is still below the 30–40% level.⁴ This is related to the fact that even for the two extreme cases of $g_A = g_V = 1$, and $g_A = 0, g_V = \sqrt{2}$ the respective shapes of L_P distribution are not dramatically different.

With the higher statistics which is already available for 7 and 8 TeV LHC and much higher statistics which will be available at 14 TeV LHC, the main factor which will affect the LHC sensitivity to the parameters g_V, g_A , is clearly the systematic error which contributed about 50% (although this might also be improved with higher statistics) in the CMS analysis at 7 TeV, 36 pb^{-1} .⁵

³Also, missing transverse momentum which is determined from the vector sum of the transverse momentum of the lepton and the jets (and used to construct $p_T(W)$) is more sensitive to PGS smearing effects for low $p_T(W)$.

⁴The panels on the r.h.s. of figures 6–8 show that the errors on g_V and g_A are closely correlated, but the error on either one is as quoted above.

⁵One should also note that at high luminosity pile-up effect will be more dramatic affecting the overall error.

So, one can expect the improvement of the sensitivity to g_V, g_A by not more than a factor of two given that the systematic error will stay the same. This would mean that the accuracy to which LHC can measure g_V, g_A couplings is quite limited and would not probably better than about 15% level unless the systematic error is decreased.

3 Conclusions

In this paper we have discussed results of the CMS collaboration on the sensitivity of the LHC to W boson polarisation in the process $pp \rightarrow W^\pm + \text{jet} \rightarrow e^\pm \text{jet} + \cancel{P}_T$ using the L_P variable.

First of all we have shown that the differential cross section for $pp \rightarrow W^\pm + \text{jet} \rightarrow e^\pm \text{jet} + \cancel{P}_T$ process with respect to L_P is sensitive to the interference between different polarizations of W -boson although it diminishes with the increase of W -boson p_T . The interference effect is of the order of the statistical experimental errors quoted in ref. [1] and presumably significantly larger than the current error bars that would be extracted from an analysis over the current (and future) entire integrated luminosity. As explained above, the template method employed in ref. [1] does take account of the interference terms in the form of a systematic uncertainty in the values of f_+, f_- and f_0 quoted with the interference terms taken to be within 10% of the Standard Model values. The results shown in Figs(2 - 4) show the entire interference effect, which is usually small but can be as large as 8% in some bins. Nevertheless, we suggest that if data with higher statistics were to be analyzed, it would be more informative simply to plot the measured differential cross-section with respect to L_p and compare this with a MC simulation that accounts directly for the interference, rather than attempt to extract values for f_+, f_- and f_0 , or alternatively to include the interference coefficients, g_{ij} into the fit procedure.

Although the sensitivity to polarisation of the W -boson was shown to be quite good — of the order of 5% as we have estimated, the sensitivity to the underlying theory in terms of g_V, g_A parameters is quite poor — of the order of 30 - 40%. The sensitivity of the LHC to (g_V, g_A) plane via the process $pp \rightarrow W^\pm + \text{jet} \rightarrow e^\pm \text{jet} + \cancel{P}_T$ is limited by systematic error and is poor even in case of statistical error is very small. The reason for this is the low sensitivity of the L_P shape variation to (g_V, g_A) . Even though, we should note that the variable L_P , suggested by CMS collaboration, is a suitable variable (and probably one of the best) to study LHC sensitivity to g_V, g_A parameters since it is directly connected to $\cos \theta^*$.

We have also found that only simulations at full detector level would allow us to fit data properly and estimate the LHC sensitivity to (g_V, g_A) parameter space. As a result of this study we have created MC generator which linked to PYTHIA generator, and can be suitably used for study of the W -boson polarisation, effects of the interference and LHC sensitivity to g_V, g_A plane. It is available upon request. This generator can produce events in the generic LHE format which can be plugged into the full detector simulation chain and used in the experimental analysis.

Our observation of the fact that the experimental sensitivity to W -boson polarization is very different and much higher than the experimental sensitivity to (g_V, g_A) parameter

space can be turned around and used to identify possible new physics at the LHC. If the $g_V - g_A$ parameter space is accurately measured from some different process and agrees with the SM predictions whilst the polarisation of the W -boson is found to be different from the SM expectations, this would be a clear indication that deviation of W -boson polarisation comes *not* from the (g_V, g_A) couplings but from different sector, such as, for example new particles with different spin statistics which would happen in case of supersymmetry.

Finally, we would like to note, that, a full NLO corrections to this process have been calculated, the QCD corrections in refs. [2, 3] and the electroweak corrections in ref. [10], but these results have not presented in terms of the variable L_p . The NLO corrections to the cross-section $d\sigma/dL_p$ would be of great interest and could well affect the results of this analysis.

Acknowledgments

We would like to acknowledge support from STFC Consolidated grant ST/J000396/1 as well as partial support from the NExT institute, a part of SEPnet. We also thank Oliver Buchmueller, Jad Marrouche and Paraskevas Sphicas for a very useful discussions and clarifications.

References

- [1] CMS collaboration, *Measurement of the polarization of w bosons with large transverse momenta in $W + jets$ events at the LHC*, *Phys. Rev. Lett.* **107** (2011) 021802 [[arXiv:1104.3829](#)] [[INSPIRE](#)].
- [2] E. Mirkes, *Angular decay distribution of leptons from W bosons at NLO in hadronic collisions*, *Nucl. Phys.* **B 387** (1992) 3 [[INSPIRE](#)].
- [3] Z. Bern et al., *Left-handed W bosons at the LHC*, *Phys. Rev.* **D 84** (2011) 034008 [[arXiv:1103.5445](#)] [[INSPIRE](#)].
- [4] ATLAS collaboration, *Measurement of the polarisation of W bosons produced with large transverse momentum in pp collisions at $\sqrt{s} = 7$ TeV with the ATLAS experiment*, *Eur. Phys. J.* **C 72** (2012) 2001 [[arXiv:1203.2165](#)] [[INSPIRE](#)].
- [5] J. Marrouche, *Triggering and W -polarisation studies with CMS at the LHC*, CERN-THESIS-2010-204 (2010).
- [6] T. Sjöstrand, *High-energy physics event generation with PYTHIA 5.7 and JETSET 7.4*, *Comput. Phys. Commun.* **82** (1994) 74 [[INSPIRE](#)].
- [7] T. Sjöstrand, S. Mrenna and P.Z. Skands, *PYTHIA 6.4 physics and manual*, *JHEP* **05** (2006) 026 [[hep-ph/0603175](#)] [[INSPIRE](#)].
- [8] J. Alwall et al., *A standard format for Les Houches event files*, *Comput. Phys. Commun.* **176** (2007) 300 [[hep-ph/0609017](#)] [[INSPIRE](#)].
- [9] J. Conway et al., *PGS 4*, <http://www.physics.ucdavis.edu/~conway/research/software/pgs/pgs4-general.htm>
- [10] S. Dittmaier, . Kramer, Michael and M. Spira, *Higgs radiation off bottom quarks at the Tevatron and the CERN LHC*, *Phys. Rev.* **D 70** (2004) 074010 [[hep-ph/0309204](#)] [[INSPIRE](#)].